X-ray Crystallography in Macromolecule

Final Report

A 9 Å Resolution X-Ray Crystallography Map of the Large Ribosomal Subunit

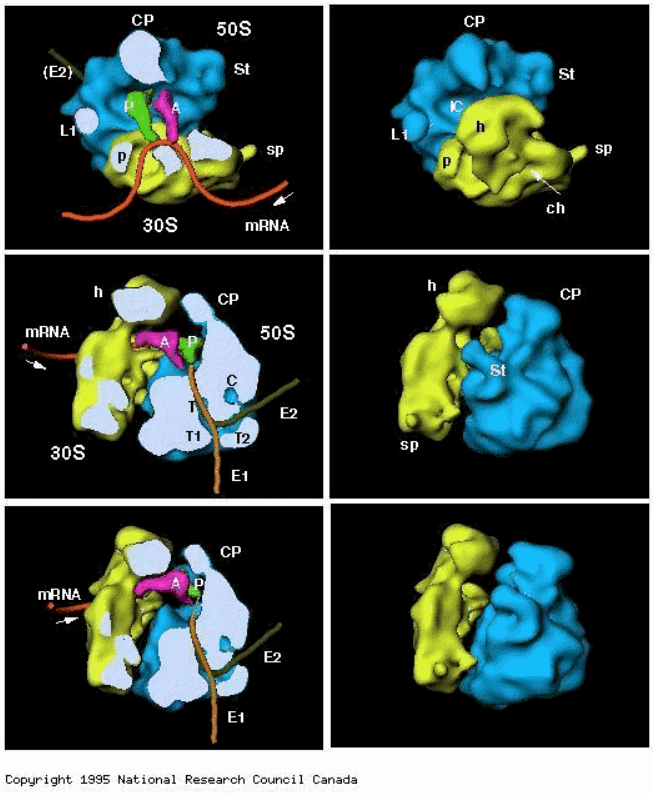

Author

Shang-Te Hsu (g874262)

http://life.nthu.edu.tw/~b830356

1999/6/28

A 9 Å Resolution X-Ray Crystallography Map of the Large Ribosomal Subunit

Cell, Vol. 93, 1105-1115, June 26, 1998

Nenad Ban[1], Betty Freeborn[2], Poul Nissen[1], Pawel Penczek[4,5], Robert A. Grassucci[4], Robert Sweet[6], Joachim Frank[4,5], Peter B. Moore[1,2], and Thomas A. Steitz[1,2,3,7]

[1]Department of Molecular Biophysics and Biochemistry

[2]Department of Chemistry

[3]Howard Hughes Medical Institute, Yale University

[4]Wadworth Center, New York State Department of Health

[5]Department of Biomedical Sciences, State University of New York

[6]Department of Biology, Brookhaven National Laboratory

Abstract

The 50S subunit of the ribosome catalyzes the peptidyl-transferase reaction of protein synthesis. The X-ray crystallographic structure of the large subunit purified from *Haloarcula marismortui* was determined up to 9 Å. The 20 Å resolution EM image reconstruction derived three dimensional structure was used as an initial phase determination to locate the positions of heavy atom cluster in three derivatives by putting it into the unit cell. The resulting structure was in agreement with the EM-derived structure at 20 Å resolution and high resolution fragment structures derived from NMR and X-ray method indicated right-handed twist of ribosomal RNA and a novel RNA-protein interaction was also found.

Introduction

In all living organisms, protein synthesis and elongation are proceeded during messenger RNA (mRNA) – peptide translation. This catalysis function undergoes in ribonecleoprotein particles called ribosomes. Ribosome has a sedimentation coefficient of about 70S and consists of two subunits: a small, 30S subunit and a large, 50S subunit. Ribosomal subunits are complexes of ribosomal RNA, rRNA and proteins. The latter has a molecular weight of about $1.5*10^6$ Da and functions as a peptide bond formation machinery. The 50S subunit contains a 2900 nt RNA and a 120 nt RNA and about 33

different proteins. Atomic resolution structures of these assembled complexes can help us to understand the mechanism of peptide bond formation and RNA-protein interactions.

Up to date, many structural studies have been derived by physical and chemical methods, such as electron microscopy (EM), neutron scattering, and X-ray crystallography. The shape and the composition of the ribosomal subunits were determined roughly by EM, the sequences and secondary such as hammer-head and loop structures of rRNA of different subunits were also determined by molecular biochemistry assay. The composition and the three dimensional spatial relation of the proteins were determined by both cryo-EM image reconstruction (**Fig.1**) and neutron scattering. However, due to the limitation of resolution and technical restriction, these results were not precise enough at atomic level.

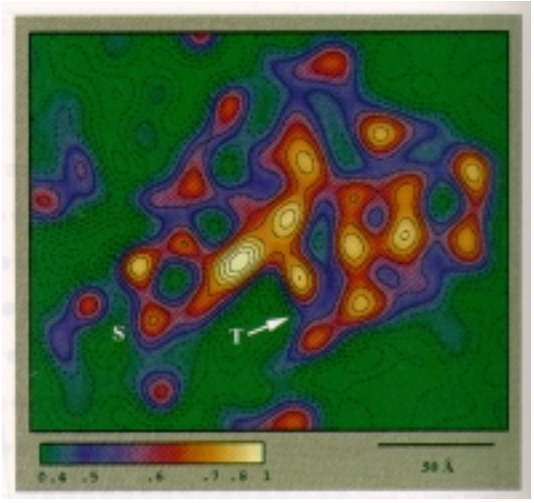

Fig 1 A color display of a single 50S ribosomal subunit highlighting the dense regions. Some of those dense regions may have high content of rRNA. Yellow color indicates high density and green color indicates low density. The protruding (labeled S) may include the stalk, identified by comparison to a low-resolution reconstruction. The arrow points to an internal low density region, which may be the entrance of the tunnel (T) which is thought to be the path of the nascent polypeptides. (*J. Mol. Biol.* (1994) **239**, 689-697

Although many high resolution crystal structures of spherical viruses, which are larger than the ribosome, have been determined during the last two decades, the structure of the ribosome is still a formidable problem to many crystallographers because of its large size and asymmetry. High symmetry of spherical viruses helped their structure determination by complexity reduction into single asymmetric unit, and thus helped the phase determination, which is the key to X-ray structures. As an approach to solve the phase problem in the ribosomal subunit, three heavy atom clusters (**Fig. 2**) were used: W18 ($(AsW_9O_{33})_2$), W11 ($Cs_5(PW_{11}O_{39}\{Rh_2(CH_3COO)_2\}$), and Ta ($Ta_6Br_{12}^{+2}$). These heavy atom clusters gave dramatically increased scattering power at low resolution, but no significant improvement at high resolution. Putting the EM-map of the *H. marismortui* large ribosomal subunit into the crystal unit cell, the locations of these heavy atom clusters were determiner by difference Patterson and difference Fourier maps (**Fig. 3**).

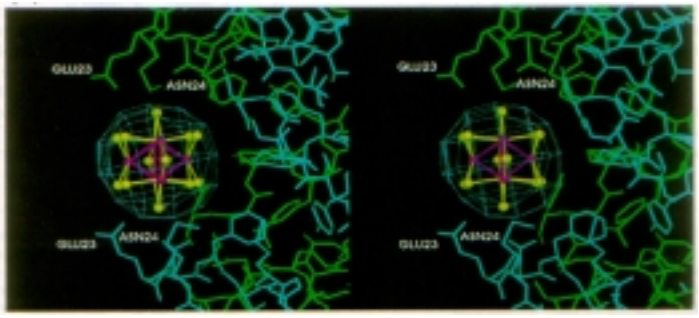

Fig. 2 Stereoplot of the $Ta_6Br_{12}^{+2}$ cluster. The structure comprises six Ta atoms (magenta) situated at the corners of a regular octahedron and twelve Br atoms (green) occupying peripheral position along the radial perpendicular bisectors.

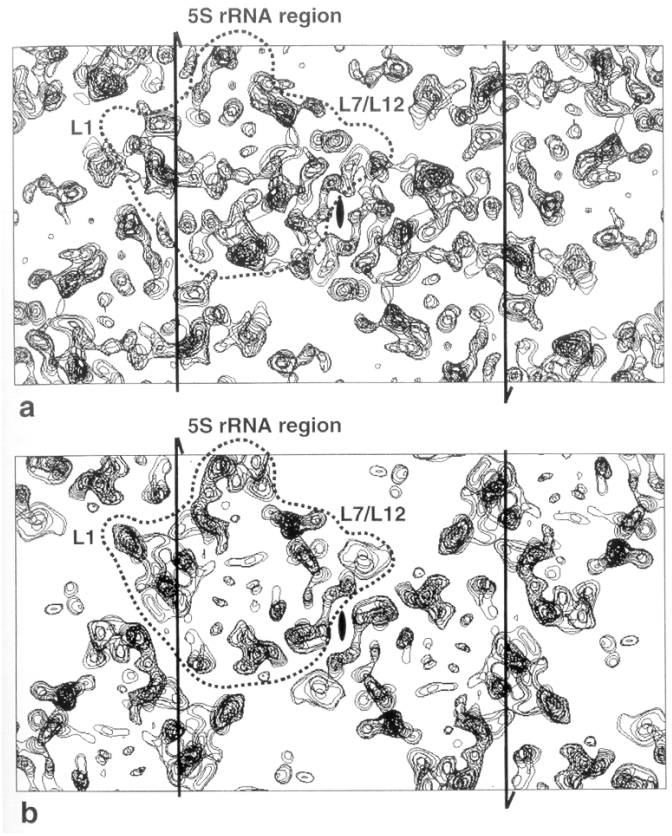

Fig 3 Comparison of HM 50S electron density maps calculated using X-ray- or EM-derived phases and X-ray amplitudes

(a) An approximately 20 Å thick superposition of sections through the HM 50S electron density map, calculated at 20 Å resolution using MIRAS X-ray phasing derived from three derivatives (**Table 2**) with no solvent flattening. The dotted line represented the 50D subunit envelope derived from the EM map positions by molecular replacement. The map shows a clear 2-fold axis and the slice through the unit cell was chosen to portray prominent features, such as the L1 region, central protuberance, and the L7/L12 region.

(b) For comparison, the superposition of the same section of a map calculated using HM 50S EM derived phases and observed X-ray diffraction amplitude is shown.

Combination of heavy atom clusters and EM-map structure phase determination, the X-ray diffraction 50S ribosomal subunit structure was determined up to 9 Å resolution by multiple isomorphous replacement and anomalous scattering (MIRAS) method. The structure revealed an atomic view of RNA helical structure and ribosomal protein L1. This result provides an insight to the structure and function of this super complex, and higher resolution will provide more detail information in the future.

Result and Discussion

The electron microscopic reconstruction of large ribosomal subunits of different species was put into the crystal unit cell (**Fig. 4**). The reconstruction was derived from 13,170 images of individual particles taken at two levels of defocus. The unit cell is orthorhombic with a space group of C221 and with unit cell dimensions of : a = 210, b = 300, c = 570 Å. The data was collected at Brookhaven National Laboratory synchrotron. After molecular replacement and rigid body refinement, the EM reconstruction of *H. marismortui* showed a better R-factor (0.39) and correlation coefficient (0.51) than *E. coli* (**Table 1**). The heavy atom derivative W18 was prepared by soaking crystals in W18 containing solution, and its difference Fourier peak increased from 13 σ to 14 σ while the R factor decrease from 44 % to 41 % for the 1322 reflections between 100 and 20 Å resolution. After MIRAS analysis for three heavy atom cluster derivatives, the major and minor occupancy sites were determined, and the quality of the phasing was excellent to 12.5 Å but dropped significantly beyond 9 Å. Therefore, a 9 Å resolution electron density map was calculated using MIRAS phasing from all three derivatives.

The overall X-ray crystallographically derived electron density map of the *H. marismortui* large ribosomal subunit at 9

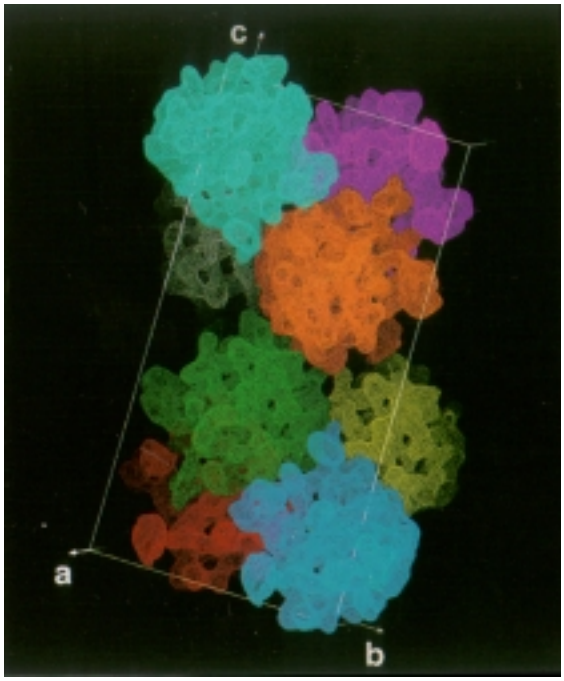

Fig. 4 The packing of *H. marismortui* 50S subunits in the orthorhombic unit cell viewed approximately down it's an axis. The eight subunits related by crystallographic symmetry are shown in different colors. Less extensive crystallographic contacts are formed between subunits colored green and orange, while green/red and orange/lavender subunit pairs have extensive contact surfaces.

Table 1. Summary of Molecular Replacement Statistics

	Correct Solution (RF)	False Peak (RF)	S/N
Direct Rotation Search (25.0–80.0 Å)			
H. marismortui	0.18	0.15	1.2
E. coli	0.20	0.22	0.92
PC Refinement of the Rotation Function Solutions (25.0–80.0 Å)			
H. marismortui	0.14	0.074	1.9
E. coli	0.14	0.087	1.6
Translation Search (25.0–80.0 Å)			
	Correct Solution (E2E2)	False Peak (E2E2)	S/N
H. marismortui	0.48	0.36	1.33
E. coli	0.44	0.35	1.26
Final Statistics (60.0–30.0 Å; 360 reflections)			
	R factor	Correlation Coefficient	
H. marismortui	0.39	0.51	
E. coli	0.45	0.43	

E2E2, Patterson correlation coefficient, where E is a normalized structure factor as defined in X-PLOR; S/N, signal to noise; RF, Rotation function value as defined in X-PLOR; R factor, $\Sigma_{hkl}(||Fobs_{hkl}| - |Fcalc_{hkl}||)/|Fobs_{hkl}|$, where $|Fobs_{hkl}|$ and $|Fcalc_{hkl}|$ are the observed and calculated structure factor amplitudes.

Table 2. Data Collection and Phasing Statistics

Data Collection

	Native	W18	W11	Ta
Soaking time		6 days	2 days	5 days
Cluster concentration (mM)		1.0	1.0	1.0
Wavelength (Å)	1.21	1.21	1.21	1.25
Resolution	100–7.2	100–7.0	100–7.0	100–7.0
Observations				
Total	98,000	204,087	191,540	15,1534
Unique	26,324	50,576	57,103	56,172
Completeness	98.3	92.7	99.2	94.2
R_{sym}	11.1	4.5	5.2	5.5
No. Sites		7	12	10
R_{iso}		23.9	27.3	19.5
$I/\sigma I$ (highest resolution bin)	11.1 (2.8)	31.7 (13.8)	24.4 (7.7)	21.6 (9.4)

MIRAS Phasing Statistics

	Resolution Shells (Å)—~6400 Reflections per Bin					
	90.0	14.2	11.3	9.9	9.0	Total (25,540 reflections)
W18						
Phasing power		1.28	1.13	0.77	0.56	1.10
R_{cullis} (centric)		0.67	0.78	0.87	0.91	0.72
W11						
Phasing power		1.4	1.2	0.85	0.63	1.15
R_{cullis} (centric)		0.65	0.78	0.83	0.88	0.70
Ta						
Phasing power		0.83	0.84	0.64	0.58	0.75
R_{cullis} (centric)		0.79	0.86	0.92	0.91	0.83
Mean figure of merit		0.82	0.71	0.54	0.43	0.63

R_{iso}: $\Sigma|F_{PH}-F_P|/\Sigma F_{PH}$, where F_{PH} and F_P are the derivative and the native structure factor amplitudes, respectively. R_{sym}: $\Sigma\Sigma_i|I_{(h)i}-I_{(h)i}|/\Sigma\Sigma_i I_{(h)i}$, where $I_{(h)}$ is the mean intensity. Phasing power: rms isomorphous difference divided by the rms residual lack of closure. R_{cullis}: $\Sigma(||F_{PH}-F_P|-|F_{H(calc)}||)/\Sigma|F_{PH}-F_P|$, where F_{PH} is the structure factor of the derivative and F_P is that of the native data. The summation is valid only for centric reflections.

Å had a spherical radius of about 250 Å and its rendering surface was very similar with the EM derived 20 Å resolution reconstruction (**Fig. 5a**). In a higher resolution, the surface structure provided more structural details, yet, the characteristics of the protruding arms, proteins (L1 and L7/L12) and rRNA segments, and mRNA penetrating cleft were almost identical as identified biochemically by immunoelectron microscopy and cryo-EM reconstruction in the early studies. Even though the 9Å resolution is not high enough to illustrate the atomic structure clearly, previous fragment X-ray and NMR structures, in another way, can greatly help picturing the huge puzzle. One example is a 5S RNA fragment solved (PDB ID 1A4D) by X-ray diffraction. The backbone structure of this RNA duplex is a standard A-form Waston-Crick base pairing, rod like structure and it can be fit in the L1 arm region attached with the L1 protein at its terminal (**Fig. 6**). Unlike the known nucleic acid-protein interaction, RNA and protein are intermingled, rather than the nucleic acid being wrapped around a protein core or encased in a protein shell. This model appears that the 50S NA ribosome structure is formed by struts of RNA rods whose branching cross-links the struts and protein acts as a stabilizing factor.

This X-ray crystallographic map of a ribosomal subunit shows electron density map expected in the previous studied. Although the quality of phasing and resolution are not good enough to identify the detail atomic coordinate, a 9 Å resolution allows a

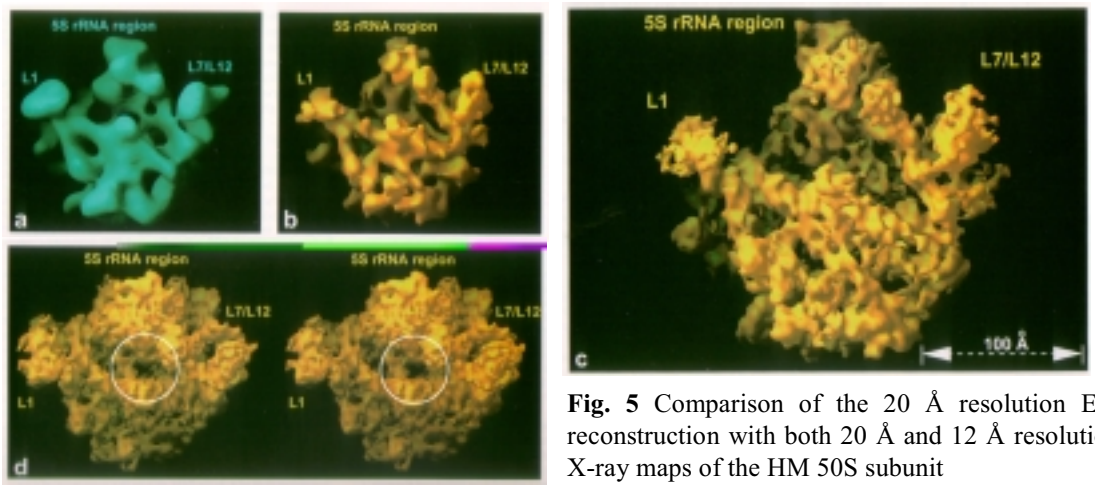

Fig. 5 Comparison of the 20 Å resolution EM reconstruction with both 20 Å and 12 Å resolution X-ray maps of the HM 50S subunit

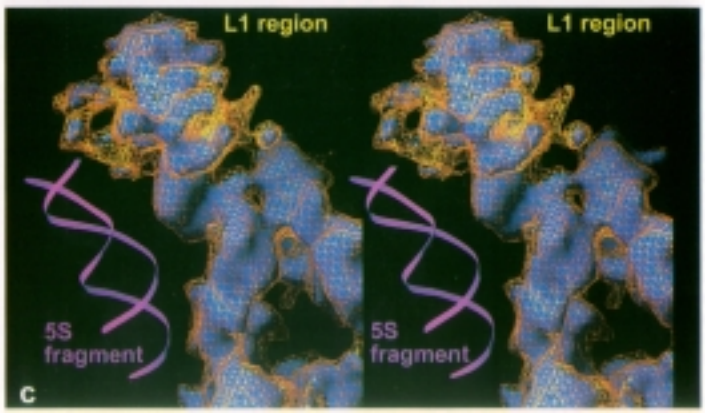

Fig. 6 A stereo close-up of a 9 Å resolution density map showing the region that includes ribosomal protein L1; a backbone ribbon model of part of the 5S RNA is shown adjacent for scale. The upper part of the density contains ribosomal protein L1, and the rest may represent rRNA that interacts with L1. The yellow cage is at a lower contour level than the solid blue.

accurate heavy atom localization and structural feature determination. As shown earlier, combining with the fragment structure results, we can still obtain a high resolution atomic structure. The further question is the mechanism and interaction of how the protein synthesis and elongation proceed among large 50S subunit, 30S small subunit and mRNA. This will rely on a higher resolution insight into it.

Reference

1. Ban N., Freeborn B., Nissen P., Penczek P., Grassucci R. A., Sweet R., Frank J., Moore P. B. & Steitz T. A. (1998) A 9 Å Resolution X-Ray Crystallography Map of the Large Ribosomal Subunit. *Cell* **93**, 1105-1115
2. Moore P. B. (1998) The three-dimensional structure of the ribosome and its components. *Annu. Rev. Biophys. Biomol. Struct.* **27**, 35-58
3. Avila-Sakar A. J., Guan T. -L., Arad T., Schmid M. F., Loke T. W., Yonath A., Piefke J., Franceschi F. & Chiu W. (1994) Electron Cryomicroscopy of *Bacillus stearothermophilus* 50S ribosomal subunits crystallized on phospholipid monolayers. *J. Mol. Biol.* **239**, 689-697

4. O'Halloran T. V., Lippard S. J., Richmond T. J. & Klung A. (1987) Multiple heavy-atom reagents for macromolecular X-ray structure determination - application of the nucleosome core particle. *J. Mol. Biol.* **194**, 705-712
5. Knäblein J., Neuefeind T., Schneider F., Bergner A., Messerschmidt A., Löwe L., Steipe B & Huber R. (1997) $Ta_6Br_{12}^{+2}$, a tool for phase determination of large biological assemblies by X-ray crystallography. *J. Mol. Biol.* **270**, 1-7
6. http://www.wadsworth.org/BMS/SCBlinks/elongation.html